Essential and mutually compensatory roles of α-mannosidase II and α-mannosidase IIx in *N*-glycan processing *in vivo* in mice

Tomoya O. Akama*, Hiroaki Nakagawa*†, Nyet Kui Wong‡, Mark Sutton-Smith‡, Anne Dell‡, Howard R. Morris‡§, Jun Nakayama¶, Shin-Ichiro Nishimura†, Ashok Pai*, Kelley W. Moremen‖, Jamey D. Marth**, and Michiko N. Fukuda*††

*Glycobiology Program, Cancer Research Center, Burnham Institute for Medical Research, La Jolla, CA 92037; †Graduate School of Advanced Life Science, Frontier Research Center for Post-Genome Science and Technology, Hokkaido University, Sapporo 001-0021, Japan; ‡Biochemistry Division of Molecular Biosciences, Imperial College, London SW7 2AZ, United Kingdom; ¶Department of Pathology, Shinshu University School of Medicine, Matsumoto 390-8621, Japan; ‖Complex Carbohydrate Research Center and Department of Biochemistry and Molecular Biology, University of Georgia, Athens, GA 30602; **Howard Hughes Medical Institute, Department of Cellular and Molecular Medicine, University of California at San Diego, La Jolla, CA 92093; and §M-SCAN Mass Spectrometry Research and Training Centre, Silwood Park, Ascot SL5 7PZ, United Kingdom

Many proteins synthesized through the secretory pathway receive posttranslational modifications, including *N*-glycosylation. α-Mannosidase II (MII) is a key enzyme converting precursor high-mannose-type *N*-glycans to matured complex-type structures. Previous studies showed that MII-null mice synthesize complex-type *N*-glycans, indicating the presence of an alternative pathway. Because α-mannosidase IIx (MX) is a candidate enzyme for this pathway, we asked whether MX functions in *N*-glycan processing by generating MII/MX double-null mice. Some double-nulls died between embryonic days 15.5 and 18.5, but most survived until shortly after birth and died of respiratory failure, which represents a more severe phenotype than that seen in single-nulls for either gene. Structural analysis of *N*-glycans revealed that double-nulls completely lack complex-type *N*-glycans, demonstrating a critical role for at least one of these enzymes for effective *N*-glycan processing. Recombinant mouse MX and MII showed identical substrate specificities toward *N*-glycan substrates, suggesting that MX is an isozyme of MII. Thus, either MII or MX can biochemically compensate for the deficiency of the other *in vivo*, and either of two is required for late embryonic and early postnatal development.

gene knockout | mutation

N-glycosylation is the major form of posttranslational modification of newly synthesized proteins through the secretory pathway. The major biosynthetic steps for *N*-glycans in vertebrates have been established (1, 2). A key conversion of high-mannose to complex-type oligosaccharides occurs in the medial Golgi, where GlcNAc-transferase I (GlcNAc-TI) adds a GlcNAc residue to form a hybrid-type *N*-glycan, GlcNAc₁Man₅GlcNAc₂ (3). Golgi α-mannosidase II (MII) then removes two mannosyl residues to form $GlcNAc_1Man_3GlcNAc_2$ (4, 5), which is further modified by GlcNAc-transferase II (GlcNAc-TII) (6) to form $GlcNAc_2Man_3GlcNAc_2$, the precursor of complex-type *N*-glycans.

When the gene encoding GlcNAc-TI was disrupted in mouse, GlcNAc-TI-null embryos died between embryonic day 9 (E9) and E10 because of defects in morphogenic processes, including the establishment of left–right asymmetry, vascularization, and neural tube formation (7, 8). The observation that GlcNAc-TI-null embryos could synthesize only high-mannose-type *N*-glycans demonstrates that high-mannose-type *N*-glycans by themselves cannot support embryonic development beyond E9–E10 in the mouse. On the other hand, mice lacking GlcNAc-TII were born and synthesized hybrid-type *N*-glycans, implying that hybrid-type *N*-glycans can support embryogenesis (9). However, GlcNAc-TII-null mice showed severe gastrointestinal, hematopoietic, osteogenic, and neuronal dysfunction, with phenotypes similar to those seen in human congenital disorders of glycosylation IIa (10, 11). This evidence indicates that hybrid-type *N*-glycans are not sufficient to maintain normal postnatal development in the mouse and in humans (12).

Although MII catalyzes the step after GlcNAc-TI and before GlcNAc-TII (1, 2), MII-null mice are born and are apparently normal except for dyserythropoiesis, causing a phenotype similar to that observed in human congenital dyserythropietic anemia type II or hereditary erythroblastic multinuclearity with a positive acidified serum lysis test (HEMPAS) (13). Furthermore, MII-nulls synthesize complex-type *N*-glycans in many tissues, despite the absence of MII enzyme activity. These findings led to the proposal of an alternative pathway for the production of complex *N*-glycans (13). Two candidate enzymes could function in this pathway; one has been reported as a cobalt-dependent broad-specificity α-mannosidase activity in rat liver microsomes (14, 15), and the other is α-mannosidase IIx (MX).

Human MX (16) is the product of the *MAN2A2* gene and is homologous to human MII, which is encoded by *MAN2A1*. Previous studies suggest that human MX is catalytically active and plays a role in *N*-glycan biosynthesis (16–18). When mouse *Man2a2*, the orthologue of human *MAN2A2*, was disrupted, MX-nulls were apparently normal, except that mutant males were subfertile (18). In the mouse testis, *N*-linked carbohydrate structures were altered compared to wild-type mice, suggesting that MX also acts to process *N*-glycans; however, the role of MX in cells other than spermatogenic germ cells remains unclear.

To determine the potential and relative role of MX in complex *N*-glycan biosynthesis *in vivo*, we generated and characterized mice lacking both *Man2a1* and *Man2a2*. We report here that double-nulls completely lack complex-type *N*-glycans and die shortly after birth. Our data further show that MX is enzymatically and functionally very similar to MII. These findings demonstrate that other enzymes cannot rescue the loss of complex *N*-glycan formation *in vivo*, thereby identifying MX activity as the compensating activity that catalyzes the alternative bypass pathway in MII-null animals.

Results

Generation of MII/MX Double-Mutant Mice. The genes encoding MII (*Man2a1*, chromosome 17E1) and MX (*Man2a2*, chromo-

BIOCHEMISTRY

some 7D1) are located on different chromosomes in the mouse, which enabled us to obtain mice lacking MII and MX genes by crossing double heterozygote *Man2a1*(+/−)/*Man2a2*(+/−) mice. However, we observed that most of the double-nulls died shortly after birth, and very few survived up to 3 weeks (Table 1, which is published as supporting information on the PNAS web site). Thus to more efficiently produce double-null pups, *Man2a1*(−/−)/*Man2a2*(+/−) mice were crossed; double-null pups resulting from this cross also showed early lethality (Table 2, which is published as supporting information on the PNAS web site). Genotyping of embryos from such crosses showed that almost all double-nulls survived until E15, some double-nulls died between E15 and the day of birth (E18), and most double-nulls died soon after birth or before postnatal day 2 (Fig. 1*A*). We also observed that many double-null neonates actively gasped for air at birth but failed to breathe properly and died, suggesting that lethality of MII/MX double-null neonates is because of respiratory failure.

Pathological Abnormalities in Double-Null Neonates and Embryos. Histological analysis indicated that lung tissue of double-null neonates had less alveolar air space by comparison to lung tissue from wild-type mice or mice mutant in either MII or MX (Fig. 1*B*). The pulmonary epithelial cell layer of double-nulls appeared thicker than that of either wild type or single-nulls, consistent with a failure of alveolar expansion in double-nulls. These morphological characteristics support the hypothesis that respiratory distress was the cause of lethality in double-null neonates. Electron microscopy of type II pneumocytes, which produce multilamellar bodies composed of surfactant proteins that prevent tissue collapse during respiration, showed abnormal vacuole formation and enlarged mitochondria in double-null animals (Fig. 1*C*).

The livers of double-nulls were also frequently damaged in neonates and E15 embryos (Fig. 1*D*). Apoptotic signals were increased in damaged areas of the double-null liver from E15 embryos, indicating increased cell death (Fig. 1*E*). Electron microscopy of the E15 liver from a double-null mouse showed abnormal vacuoles and enlarged mitochondria (Fig. 1*F*), characteristics also seen in the lungs of double-nulls (Fig. 1*C*). Similar abnormal vacuoles and enlarged mitochondria were seen in proximal tubule cells of the double-null kidney. However, these abnormal morphologies were not apparent in other tissues, such as heart, small intestine, and pancreas, in double-null mice (Fig. 7, which is published as supporting information on the PNAS web site), suggesting that the appearance of vacuoles and enlarged mitochondria is cell-type-dependent.

Absence of Complex-Type *N*-Glycans in Double-Null Embryos. Lectin blot analysis showed that lens culinaris agglutinin (LCA) lectin, which binds to high-mannose-type *N*-glycans, reacted strongly with membrane proteins from all genotypes (Fig. 2*A*). LCA lectin also reacted with tissue sections of E15 wild-type and double-null embryos (Fig. 2*B*). By contrast, both leukocyte (L-)phaseolus vulgaris agglutinin (PHA) and erythrocyte (E-)PHA, which are specific for complex-type *N*-glycans, reacted strongly with wild type and MX-nulls, weakly with MII-nulls, and not at all with double-nulls. These results strongly suggest that double-null embryos have no complex-type *N*-glycans.

MALDI-TOF MS (Fig. 3) showed that the *N*-glycans from both wild-type and MX-null mice are mainly complex-type. They also contained high-mannose-type but not significant levels of hybrid-type *N*-glycans. In contrast, MII-null embryos showed high levels of hybrid-type *N*-glycans and reduced levels of complex-type *N*-glycans, whereas in double-null embryos, signals
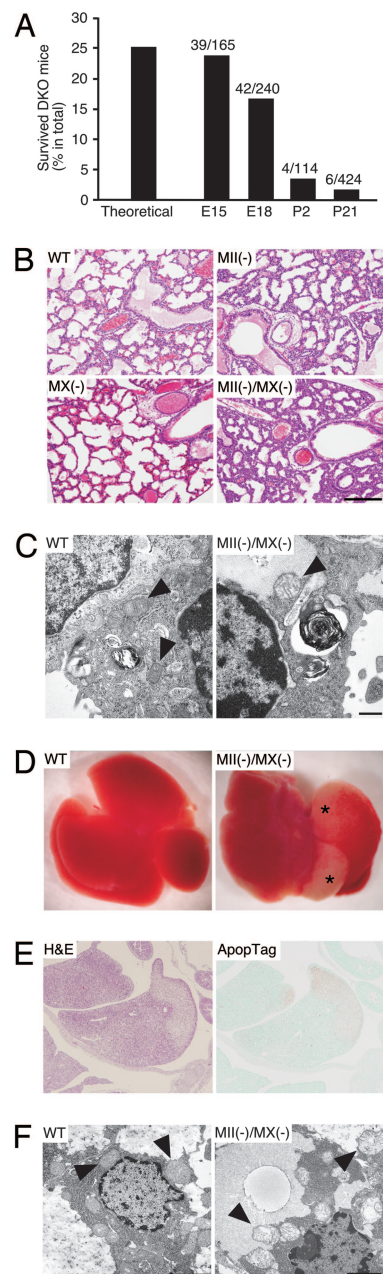

Fig. 1. Survival of MII/MX double-nulls during embryonic and postnatal development and morphological analysis of double-nulls. (*A*) Survival rate of MII/MX double-nulls during embryonic and postnatal development. *Man2a1*(−/−)/*Man2a2*(+/−) mice were crossed, and embryos obtained from pregnant female mice and postnatal pups were genotyped. Each bar represents the relative numbers of surviving double-null embryos and neonates per total offspring. (*B*) Histological observation of neonatal mouse lung. Hematoxylin/eosin (H&E) staining of paraffin-embedded tissue sections demonstrated that the double-null neonatal lungs have less air space and thicker alveolar septa. (Scale bar, 200 μm.) (*C*) Electron micrographs of alveolar type II pneumocytes from wild-type and MII/MX double-null animals. Note the presence of large vacuoles and enlarged mitochondria in the double-nulls (mitochondria in both pictures are indicated by arrowheads). (Scale bar, 500 nm.) (*D*) Macroscopic observation of neonatal livers. Apparent abnormalities in the double-null liver are marked by asterisks. (*E*) Apoptosis analysis of cells from MII/MX double-null liver. Paraffin-embedded section of double-null E15 embryo displayed signs of massive apoptosis in liver, correlated with paler H&E staining. (*F*) Electron micrographs of hepatocytes from wild-type and MII/MX double-null embryos at E15. Mitochondria in both pictures are indicated by arrowheads. Note that the double-null hepatocyte contains large vacuoles and enlarged mitochondria, similar to observations of lung type II pneumocytes (*C*). (Scale bar, 2 μm.)
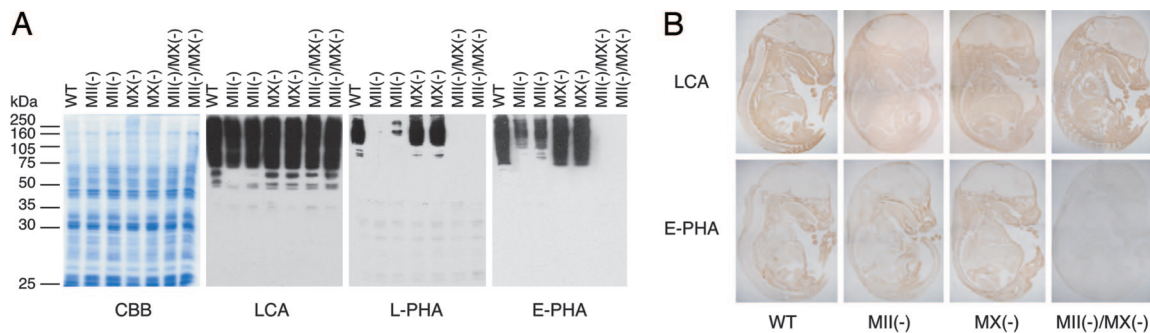
Fig. 2. Lectin blot and lectin histochemistry of mouse embryos. (*A*) Lectin blot of membrane proteins from E15 embryos. Shown are an SDS/PAGE gel stained with Coomassie blue (CBB) for total protein and blots probed with lens culinaris agglutinin (LCA), leukocyte PHA, and E-PHA lectins. (*B*) Lectin histochemistry of E15 embryos. Paraffin sections of each embryo were probed with LCA or E-PHA lectins.

for hybrid-type *N*-glycans were significantly increased, and complex-type *N*-glycans had completely disappeared.

2D-HPLC analysis (19, 20) (Fig. 4) of *N*-glycans from E15 embryos showed that complex-type structures constituted >40% of total *N*-glycans in wild-type and MX-null embryos, whereas in MII-nulls, complex-type *N*-glycans were reduced to 15%. Strikingly, complex-type *N*-glycans were completely absent in

MII/MX double-null embryos, which is consistent with the results of the lectin blots and MALDI-TOF analysis (Fig. 3). Moreover, hybrid-type *N*-glycans, which were not found in wild-type and MX-null mice, were the major population in MII/MX double nulls, indicating that these uncommon structures had accumulated in the double-nulls. Embryos from all genotypes did not show significant quantitative differences in
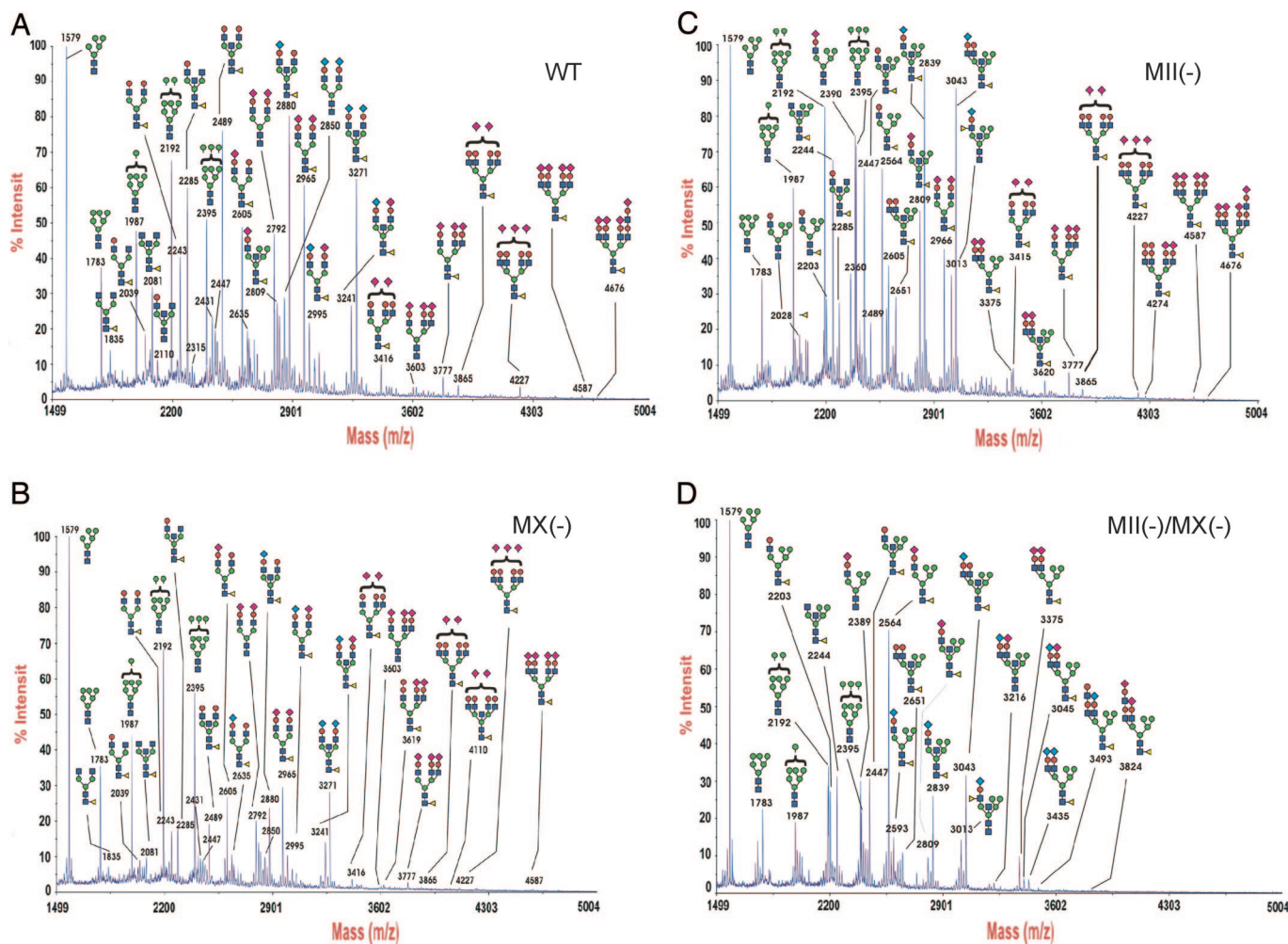

Fig. 3. MALDI-TOF analysis of *N*-glycans from E15 embryos. (*A*) Wild type, (*B*) MX-null, (*C*) MII-null, and (*D*) MII/MX double-null. *N*-glycans were released from embryo homogenates by peptide *N*-glycosidase F digestion and were permethylated before MALDI-TOF analysis. Annotations are based on compositional information provided by MALDI molecular weights, complemented by collisional activation tandem MS and linkage analysis experiments (data not shown).
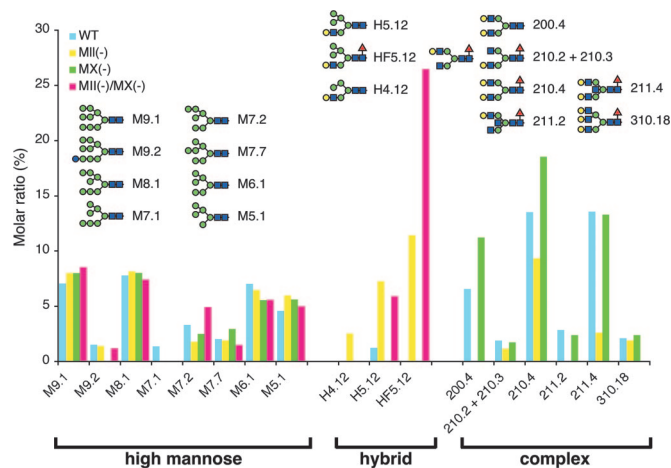
Akama *et al.*

Fig. 4. 2D-HPLC analysis of N-glycans from E15 embryos. A summary of the quantitative glycan analysis is presented. The nomenclature of N-glycans has been described (19, 34). Original data of HPLC profiles are available upon request.
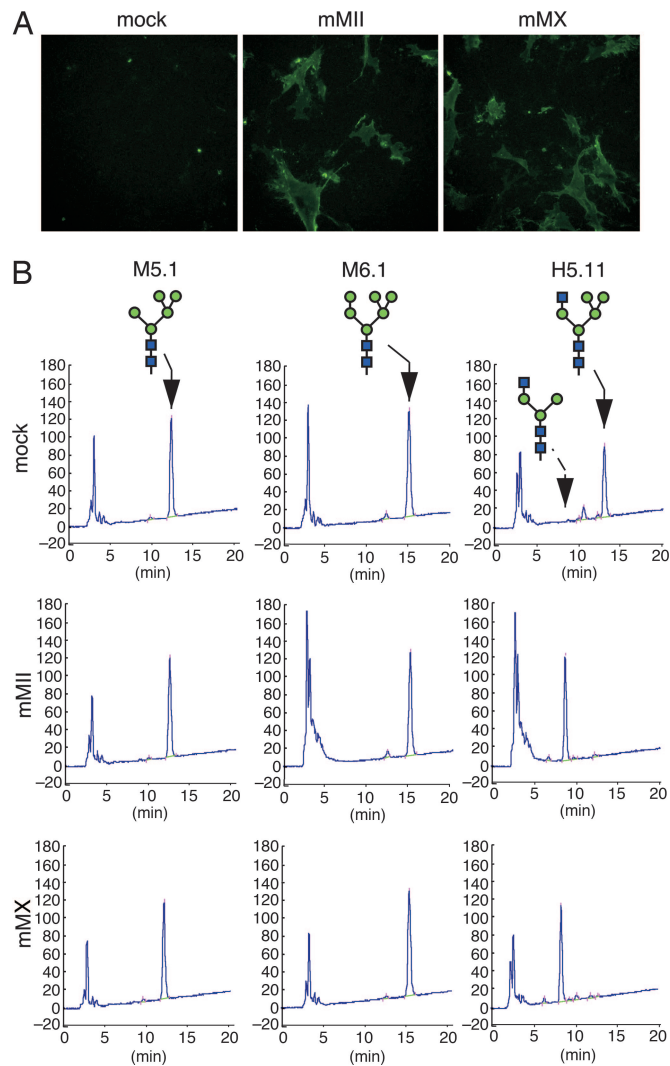

Fig. 5. Enzymatic activity of recombinant MX in vivo and in vitro. (A) Rescue of complex-type N-glycan synthesis by α-mannosidases in MII/MX double-null fibroblasts. MII/MX double-null fibroblasts were transfected with vector alone (mock), vector encoding mouse MII cDNA (mMII), or vector encoding mouse MX cDNA (mMX). Transfected cells were probed with E-PHA lectin to detect complex-type N-glycans. (B) Enzymatic hydrolysis of N-glycan oligosaccharides with recombinant α-mannosidases. Each PA-tagged oligosaccharide, M5.1, M6.1, and H5.11 was incubated with a soluble form of the respective enzyme synthesized and secreted from COS-1 cells, and the digest was analyzed by amide-column HPLC. The elution position of the starting material and final product (100.2) is shown by the solid and dashed arrows, respectively.

high-mannose-type N-glycans. Based on these results presented in Figs. 2–4, we conclude that MX functions in N-glycan processing *in vivo* in the mouse, and that lack of both MII and MX leads to arrest of N-glycan processing at hybrid-type structures.

Enzymatic Activity of Mouse MX. To further evaluate the enzymatic activity of MX in N-glycan processing, we asked whether recombinant MX could rescue synthesis of complex-type N-glycans in double-null cells. MII/MX double-null fibroblasts failed to react with E-PHA lectin, presumably because of the absence of complex-type N-glycans (Fig. 5A, mock). When mouse MII cDNA was transfected into these fibroblasts, transfected cells became reactive to E-PHA, confirming MII activity *in vivo* in N-glycan processing (Fig. 5A, mMII). When full-length mouse MX cDNA was transfected into double-null fibroblasts, transfected cells also became reactive to E-PHA (Fig. 5A, mMX), indicating that mouse MX functions in the processing step in a manner similar to MII.

To determine whether mouse MX can hydrolyze an oligosaccharide substrate *in vitro*, we produced soluble recombinant MX in COS cells. Soluble MX was then incubated with 2-aminopyridine (PA)-tagged N-glycans, and products were analyzed by HPLC (Fig. 5B). The results showed that MX specifically removes two mannosyl residues from $GlcNAc_1Man_5GlcNAc_2$ (H5.11) to produce $GlcNAc_1Man_3GlcNAc_2$ (100.2), whereas it showed no reactivity to high-mannose-type carbohydrates M5.1 and M6.1. These results demonstrate that MX specifically hydrolyzes the same oligosaccharide substrate as does MII, indicating that MX is an isozyme of MII.

Discussion

The aim of this study was to determine whether MX was responsible for the alternative pathway of complex N-glycan formation previously described in MII-deficient mice (13). The data presented here indicate an absence of complex-type N-glycans in MII/MX double-null mice (Figs. 2–4), demonstrating that MX is the only enzyme able to compensate for the absence of the MII step in N-glycan processing *in vivo*. These observations are consistent with the absence of any other genes closely related to either *Man2a1* (MII) or *Man2a2* (MX) within the Class 2 (glycosylhydrolase family 38) α-mannosidases (21) in human or mouse genome databases (22). These data also exclude a role for the Co^{2+}-stimulated broad-specificity

α-mannosidase activity previously termed α-mannosidase III (13) in N-glycan biosynthesis. This latter enzyme has previously been identified in BHK cells and rat liver and has been shown to cleave $Man_{9-4}GlcNAc_2$ to $Man_3GlcNAc_2$ without the requirement for GlcNAc-TI activity (14, 15). As our data (Fig. 5) showed, MX removes two α-mannosyl residues from $GlcNAc_1Man_5GlcNAc_2$ to produce $GlcNAc_1Man_3GlcNAc_2$ but does not cleave $Man_{6-5}GlcNAc_2$, suggesting that MX is an isozyme of MII. Based on these findings, we propose a revision in the previously described N-glycan processing pathway (13), as shown in Fig. 6.

When full-length mouse MX was additionally expressed in MII/MX double-null fibroblasts, transfected cells produced complex-type N-glycans (Fig. 5A), indicating that full-length MX can rescue the complex N-glycan deficiency in double-null cells.
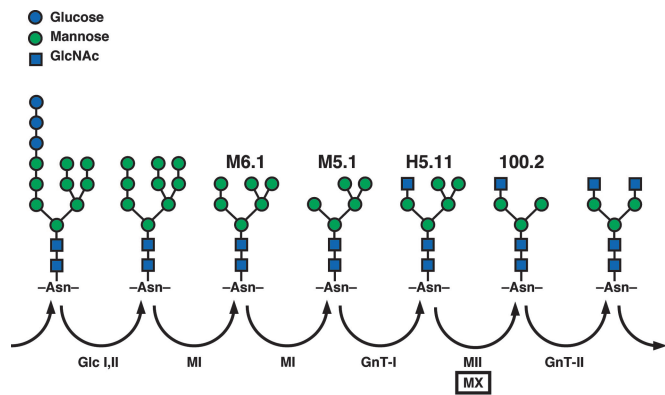
Fig. 6. The *N*-glycan processing pathway, including MX. This study demonstrates that MII and MX are isozymes hydrolyzing the hybrid-type H5.11 structure, and that either enzyme is required for formation of complex-type *N*-glycans. This study also excludes the likelihood of an alternative processing pathway catalyzed by a different enzyme capable of bypassing this critical processing step in MII/MX double-null mice.

In vitro enzyme assays using the soluble catalytic domain of MX also detected activity toward a $GlcNAc_1Man_5GlcNAc_2$ substrate in contrast to prior studies using a recombinant form of human MX (17). We recently identified alternatively spliced forms and sequence polymorphisms of human MX and confirmed that several of these transcripts encode enzymes active toward $GlcNAc_1Man_5GlcNAc_2$, whereas a splice variant used in our previous study (17) was not active toward high-mannose oligosaccharides or $GlcNAc_1Man_5GlcNAc_2$ (H. Singh, T.O.A., M.N.F., and K.W.M., unpublished data).

Although MX and MII target the same substrate, MX-null mouse tissues do not accumulate oligosaccharides such as H5.12 and HF5.12 (Fig. 4). Western blot analysis of MX in wild-type mice detected a 160-kDa MX protein in the testis (18), whereas this species was not detected in other tissues examined, suggesting that expression levels of active MX are minimal in most tissues other than testis. This observation may explain why MII-like mannosidase activity was not detected in MII-null liver (13). However, despite such low expression levels, the existence of MX activity in tissues other than testis is evidenced by the ability of those tissues derived from the MII-null mouse to synthesize complex-type *N*-glycans. It is likely that, in many cell types, MII rather than MX is the major contributor to *N*-glycan processing. Because MX-null animals showed *N*-glycan patterns similar to those seen in wild-type mice (Figs. 2–4), MX may play a subsidiary role in *N*-glycan processing in many mouse tissues.

MII/MX double-null mice exhibit lethality shortly after birth (Fig. 1*A*), presumably because of respiratory failure. A thickened epithelial cell layer and corresponding decrease in alveolar air space was observed in the lungs of double-null animals along with abnormal vacuolation and enlarged mitochondria in alveolar type II pneumocytes (Fig. 1*B*). In the lung, type II pneumocytes have a primary role in the synthesis and secretion of surfactant proteins and phospholipids from cytoplasmic multilamellar bodies (23). Pulmonary surfactants in the lung have been shown to reduce surface tension, aid in alveolar expansion, and prevent alveolar collapse during respiration. Mutant mice deficient in surfactant proteins display altered surfactant homeostasis and in some cases severe respiratory failure (24–27). In human newborns, deficiency in multilamellar bodies is also associated with respiratory failure (28). Because multilamellar bodies are produced in the lysosome from tightly packed precursor bodies through proteolytic digestion, the integrity of lysosomes may be critical for their biogenesis. Indeed, increased glycosylation of lysosomal membrane proteins, such as the

lysosome-associated membrane proteins (LAMPs) (29), through acquisition of $\beta1,6GlcNAc$ branching and polylactosamine extension, results in elevated production of multilamellar bodies (30). We observed that levels of polylactosamine-extended LAMP proteins, particularly LAMP2, were reduced in tissues from MX/MII double-nulls (T.O.A. and M.N.F., unpublished data). Therefore, underprocessing of *N*-glycans associated with LAMPs may contribute to a failure in the protection of lysosomes against proteolytic digestion in double-null animals, which may lead to inefficient multilamellar body formation. Further studies should address the roles of *N*-glycan processing in surfactant biogenesis and lung pathology in the double-null mice.

A recent report described the perinatal lethality phenotype of the $\alpha1,6$-fucosyltransferase (*Fut8*)-null mouse, which is defective in core *N*-glycan fucosylation. Similar to the MII/MX double-nulls, *Fut8*-null mice die shortly after birth because of abnormal lung development (31). In contrast to the constricted alveoli and thickened alveolar epithelial layer seen in MII/MX double-nulls (Fig. 1*B*), the lungs from *Fut8*-null mice show enlarged alveoli. Deficiency in *Fut8* results in overexpression of metalloproteases and excessive degradation of extracellular matrix, which is attributed to dysregulation of $TGF\beta$ signaling. Although there is a significant contrast in the histologies of these two mouse mutants, these studies indicate that proper *N*-glycosylation is essential for lung development and survival of newborn mice.

It is striking that the phenotypes of MII/MX double-null mice fall between those of the GlcNAc-TI- and GlcNAc-TII-null animals. Embryonic lethality around E9–E10 was observed in GlcNAc-T1-nulls (7, 8), whereas neonatal lethality was seen in MII/MX double-nulls (this study), and early postnatal lethality (1–4 weeks after birth), depending on genetic background, was observed in GlcNAc-TII-nulls (9). Thus, a graded severity of lethal phenotypes is seen, depending on which step in the *N*-glycan processing pathway is disrupted. These findings clearly indicate the importance of *N*-glycan maturation and extension and the formation of complex-type structures to normal mouse development. This present study also identifies the only two $\alpha3,6$-mannosidases capable of providing a processing route to complex-type *N*-glycan structures in animal systems.

Materials and Methods

Production of Man2a1(−/−)/Man2a2(−/−) Double-Null Mice. *Man2a1*(−/−) (13) and *Man2a2*(−/−) mice (18) were mated. Resulting *Man2a1*(+/−)/*Man2a2*(+/−) mice were then crossed to obtain double-null animals. For genotyping, PCR analysis of each allele was performed by using allele-specific primers (sequences are listed in *Supporting Text*, which is published as supporting information on the PNAS web site) with tail biopsy DNA as a template. To analyze the survival rate of double-null mice at embryonic and neonatal stages, *Man2a1*(−/−)/*Man2a2*(+/−) mice were crossed, and embryos were recovered at defined time points. Embryos or isolated tissues were either fixed in 4% paraformaldehyde in PBS or stored at −80°C until use.

Lectin Blot and Lectin Histochemistry. Detailed information on lectin blotting and histochemistry is available in *Supporting Text*. In brief, membrane fractions obtained from whole E15 embryos were subjected to SDS/PAGE, and the proteins were transferred to poly(vinylidene difluoride) filters. After blocking with BSA, the filter was incubated with 2.5 μg/ml biotinylated lectin (Vector Laboratories) for 1 h at room temperature, unbound lectin was removed by washing, and the blots were subsequently incubated with horseradish peroxidase- (HRP) avidin for 30 min. After washing, bound HRP on the filter was visualized by using the SuperSignal West Pico Kit (Pierce Biotech). For lectin

BIOCHEMISTRY

histochemistry, thin sections from a paraffin-embedded E15 embryo were subjected to lectin analysis as described above, except diaminobenzidine was used for signal detection.

Construction of Expression Vectors for MII and MX Enzymes. DNA fragments encoding full-length or soluble forms of mouse MII and MX were amplified from a mouse brain cDNA library (BD Biosciences, Palo Alto, CA) by PCR (see *Supporting Text* for detailed procedure). After confirmation of the sequences, DNA fragments encoding full-length enzymes were subcloned into the pcDNA3.1 mammalian expression vector (Invitrogen). cDNA fragments encoding soluble forms of enzymes were subcloned into pcDNA-HSH (32).

Recombinant Protein Expression in Cultured Cells. An expression vector encoding either MII or MX was transfected into cultured cells by using LipofectAMINE Plus reagent (Invitrogen), as recommended by the manufacturer. Transfected cells were cultured for 2 days and subjected to lectin cytochemistry or used for soluble enzyme preparation.

Mannosidase Activity Assay. Fifteen picomoles of a PA-tagged oligosaccharide was incubated with 3 μl of concentrated medium containing the soluble form of the respective enzyme (see *Supporting Text* for preparation) in 50 μl of 100 mM sodium acetate buffer, pH 5.8, at 37°C for 20 h. The reaction was stopped by boiling for 5 min, and the product was analyzed by 2D-HPLC analysis.

2D-HPLC Analysis of PA-Derivatized *N*-Glycans. Mouse embryos were homogenized in 0.1 M NH$_4$OAc and boiled for 15 min, followed by lyophilization. The samples were next suspended in 50 mM

Tris·HCl/10 mM CaCl$_2$, pH 8.0, and digested with trypsin and chymotrypsin (Sigma) at 37°C for 16 h. After inactivation of the enzymes by boiling, samples were treated with peptide *N*-glycosidase F (Roche Diagnostics) at 37°C for 16 h, and released *N*-glycans were purified by gel filtration chromatography and subsequently subjected to fluorescent labeling with PA (33). PA-derivatized *N*-glycans were again purified by using gel filtration, desialylated, and analyzed by 2D mapping (34) by using reverse-phase HPLC followed by amide-column HPLC.

MALDI-TOF Analysis of Permethylated *N*-Glycans. Embryos were homogenized on ice in extraction buffer containing 0.5% wt/vol SDS/0.1 M Tris·HCl, pH 7.4. After dialysis and lyophilization, extracts were reduced and carboxymethylated followed by sequential tryptic and peptide *N*-glycosidase F digestion and Sep-Pak purification. MALDI-TOF data were acquired by using a Voyager-DE STR mass spectrometer (Applied Biosystems) in the reflectron mode with delayed extraction. Permethylated samples were dissolved in 10 μl of methanol, and 1 μl of each dissolved sample was premixed with 1 μl of matrix (2,5-dihydrobenzoic acid) before loading onto a metal plate.

1. Kornfeld, R. & Kornfeld, S. (1985) *Annu. Rev. Biochem.* **54,** 631–664.
2. Schachter, H. (1991) *Glycobiology* **1,** 453–461.
3. Schachter, H., Narasimhan, S., Gleeson, P. & Vella, G. (1983) *Can. J. Biochem. Cell Biol.* **61,** 1049–1066.
4. Tulsiani, D. R., Hubbard, S. C., Robbins, P. W. & Touster, O. (1982) *J. Biol. Chem.* **257,** 3660–3668.
5. Moremen, K. W., Trimble, R. B. & Herscovics, A. (1994) *Glycobiology* **4,** 113–125.
6. Harpaz, N. & Schachter, H. (1980) *J. Biol. Chem.* **255,** 4885–4893.
7. Ioffe, E. & Stanley, P. (1994) *Proc. Natl. Acad. Sci. USA* **91,** 728–732.
8. Metzler, M., Gertz, A., Sarkar, M., Schachter, H., Schrader, J. W. & Marth, J. D. (1994) *EMBO J.* **13,** 2056–2065.
9. Wang, Y., Tan, J., Sutton-Smith, M., Ditto, D., Panico, M., Campbell, R. M., Varki, N. M., Long, J. M., Jaeken, J., Levinson, S. R., *et al.* (2001) *Glycobiology* **11,** 1051–1070.
10. Tan, J., Dunn, J., Jaeken, J. & Schachter, H. (1996) *Am. J. Hum. Genet.* **59,** 810–817.
11. Schachter, H. & Jaeken, J. (1999) *Biochim. Biophys. Acta* **1455,** 179–192.
12. Wang, Y., Schachter, H. & Marth, J. D. (2002) *Biochim. Biophys. Acta* **1573,** 301–311.
13. Chui, D., Oh-Eda, M., Liao, Y. F., Panneerselvam, K., Lal, A., Marek, K. W., Freeze, H. H., Moremen, K. W., Fukuda, M. N. & Marth, J. D. (1997) *Cell* **90,** 157–167.
14. Bonay, P. & Hughes, R. C. (1991) *Eur. J. Biochem.* **197,** 229–238.
15. Bonay, P., Roth, J. & Hughes, R. C. (1992) *Eur. J. Biochem.* **205,** 399–407.
16. Misago, M., Liao, Y. F., Kudo, S., Eto, S., Mattei, M. G., Moremen, K. W. & Fukuda, M. N. (1995) *Proc. Natl. Acad. Sci. USA* **92,** 11766–11770.
17. Oh-Eda, M., Nakagawa, H., Akama, T. O., Lowitz, K., Misago, M., Moremen, K. W. & Fukuda, M. N. (2001) *Eur. J. Biochem.* **268,** 1280–1288.
18. Akama, T. O., Nakagawa, H., Sugihara, K., Narisawa, S., Ohyama, C., Nishimura, S., O'Brien, D. A., Moremen, K. W., Millan, J. L. & Fukuda, M. N. (2002) *Science* **295,** 124–127.
19. Takahashi, N., Nakagawa, H., Fujikawa, K., Kawamura, Y. & Tomiya, N. (1995) *Anal. Biochem.* **226,** 139–146.
20. Takahashi, N. & Tomiya, N. (1992) in *Analysis of N-Linked Oligosaccharides: Application of Glycoamidase A,* eds. Takahashi, N. & Muramatsu, T. (CRC, Boca Raton, FL), pp. 199–332.
21. Henrissat, B. & Davies, G. (1997) *Curr. Opin. Struct. Biol.* **7,** 637–644.
22. Park, C., Meng, L., Stanton, L. H., Collins, R. E., Mast, S. W., Yi, X., Strachan, H. & Moremen, K. W. (2005) *J. Biol. Chem.* **280,** 37204–37216.
23. Haagsman, H. P. & van Golde, L. M. (1991) *Annu. Rev. Physiol.* **53,** 441–464.
24. Botas, C., Poulain, F., Akiyama, J., Brown, C., Allen, L., Goerke, J., Clements, J., Carlson, E., Gillespie, A. M., Epstein, C. & Hawgood, S. (1998) *Proc. Natl. Acad. Sci. USA* **95,** 11869–11874.
25. Clark, J. C., Wert, S. E., Bachurski, C. J., Stahlman, M. T., Stripp, B. R., Weaver, T. E. & Whitsett, J. A. (1995) *Proc. Natl. Acad. Sci. USA* **92,** 7794–7798.
26. Glasser, S. W., Burhans, M. S., Korfhagen, T. R., Na, C. L., Sly, P. D., Ross, G. F., Ikegami, M. & Whitsett, J. A. (2001) *Proc. Natl. Acad. Sci. USA* **98,** 6366–6371.
27. Korfhagen, T. R., Bruno, M. D., Ross, G. F., Huelsman, K. M., Ikegami, M., Jobe, A. H., Wert, S. E., Stripp, B. R., Morris, R. E., Glasser, S. W., *et al.* (1996) *Proc. Natl. Acad. Sci. USA* **93,** 9594–9599.
28. Cutz, E., Wert, S. E., Nogee, L. M. & Moore, A. M. (2000) *Am. J. Respir. Crit. Care Med.* **161,** 608–614.
29. Fukuda, M. (1991) *J. Biol. Chem.* **266,** 21327–21330.
30. Hariri, M., Millane, G., Guimond, M. P., Guay, G., Dennis, J. W. & Nabi, I. R. (2000) *Mol. Biol. Cell* **11,** 255–268.
31. Wang, X., Inoue, S., Gu, J., Miyoshi, E., Noda, K., Li, W., Mizuno-Horikawa, Y., Nakano, M., Asahi, M., Takahashi, M., Uozumi, N., *et al.* (2005) *Proc. Natl. Acad. Sci. USA* **102,** 15791–15796.
32. Angata, K., Yen, T.-Y., El-Battari, A., Macher, B. A. & Fukuda, M. (2001) *J. Biol. Chem.* **276,** 15369–15377.
33. Hase, S., Ikenaka, T. & Matsushima, Y. (1978) *Biochem. Biophys. Res. Commun.* **85,** 257–263.
34. Tomiya, N., Awaya, J., Kurono, M., Endo, S., Arata, Y. & Takahashi, N. (1988) *Anal. Biochem.* **171,** 73–90.